Electronic Supplementary Information

Plasmonic photo-current in freestanding monolayered gold nanoparticle membranes

Mélanie Gauvin[a], Thomas Alnasser[a], Elie Terver[a,b], Inés Abid[b], Adnen Mlayah[b], Shenqui Xie[c], Juergen Brugger[c], Benoit Viallet[a], Laurence Ressier[a], Jérémie Grisolia[a*],

[*]: jeremie.grisolia@insa-toulouse.fr

[a] Université de Toulouse, LPCNO, INSA-CNRS-UPS, 135 avenue de Rangueil, Toulouse 31077, France.
[b] CEMES-CNRS and Université de Toulouse, 29 rue Jeanne Marvig, BP 94347, F-31055 Toulouse Cedex 4, France
[c] Microsystems Laboratory, École Polytechnique Fédérale de Lausanne, Station 17, 1015 Lausanne, Switzerland

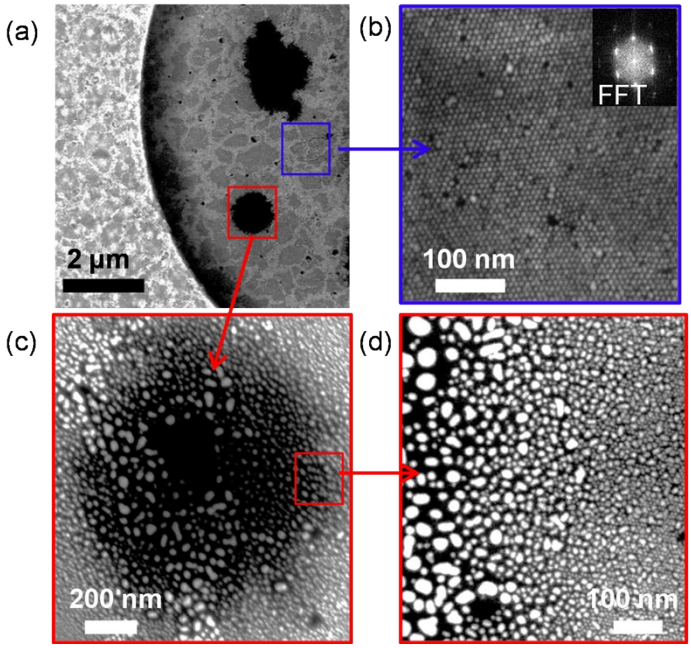

Figure S1: SEM observations of a NP membrane: (a) View from inside and outside the NP membrane. (b) View of the long range order assembly of Au NPs in an hexagonal compact network, as confirmed by the fast Fourier transform (FFT) pattern. (c) View of a region inside the membrane where the NP array has coalesced after high I_{Laser} exposure (15mW at 5% with spot =1.9µm^2, I_{Laser}~40kW/cm^2) –the coalesced region has a diameter close to the laser spot size. (d) Zoom-in of the boundary of the exposition zone: the frontier between intact and coalesced nanoparticles is clearly visible.

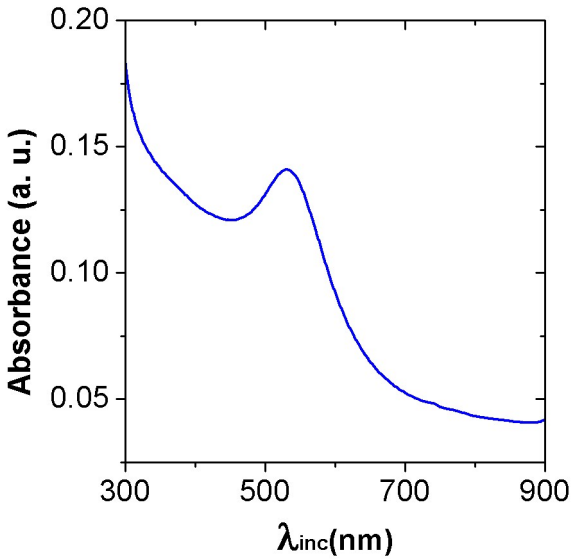

Figure S2: Absorption spectrum of dodecanethiol coated 7 nm Au nanoparticles in toluene with single surface plasmon resonance at λ_{inc} = 528 nm.

Discrete dipole appromixation (DDA) simulations

The simulations of the optical extinction spectra and electric near-field were performed using the ddscat 7.3 software by Draine and Flatau.[1-4] The positions and sizes of each of the 350 nanoparticles of the TEM image (Figure S3a) were extracted assuming spherical nanoparticles. Then, each nanoparticle was described by around 2000 point dipoles distributed on a cubic lattice with 0.5 nm inter-dipole separation for which a full convergence of the calculations was obtained. The optical constants (n, k) of gold were taken from reference 5 and the optical index 1.46 of dodecanethiol was assumed for the surrounding medium.

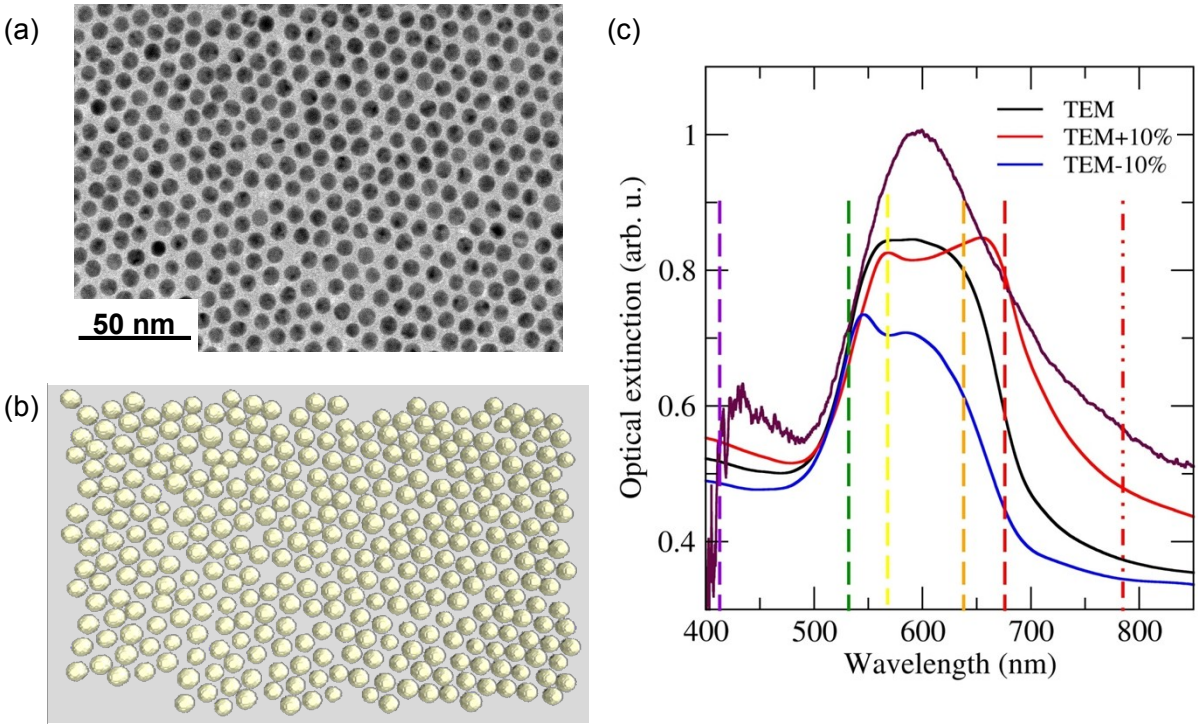

Figure S3: (a) Transmission electron microscopy image of a freestanding monolayered Au NP membrane. (b) Discrete Dipole Approximation (DDA) target of nano-sphere array built upon a realistic array as shown in (a). (c) Experimental optical absorption of a freestanding Au NP membrane (purple curve) and simulated optical absorption spectra of a monolayered array of Au NPs embedded in dodecanethiol matrix (n=1.46) based on target (b) using a DDA code. The black curve indicates the DDA simulation done with nanoparticle positions and size distribution as shown in TEM image (a). The blue and red curves indicate the simulation results obtained with + 10% and -10% in the mean nanoparticle size, respectively.

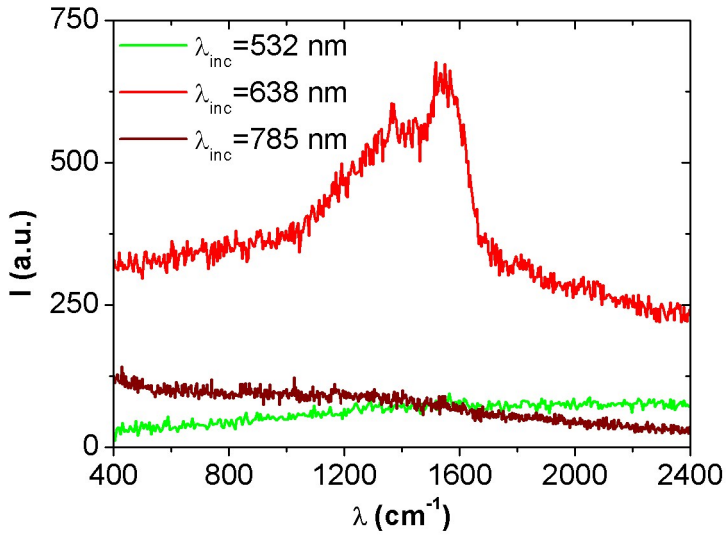

Figure S4: Raman spectra of a freestanding Au NP membrane at different excitation wavelengths λ_{inc} = 532 nm (green curve), 638 nm (red curve), 785 nm (brown curve).

Electron transport measurements:

Transport measurements were performed using a Keithley 4200-SCS DC characterization system and a cryogenic probe station (Janis ST-500-1) working at 10^{-5} mbar in the temperature range 79–300 K. The Keithley 4200–SCS DC characterization system was equipped with a Keithley SMU pre-amp, which gives a base level of approximately 1 fA with triax connections. The temperature-dependent electrical dark electrical conductance $G_{dark}(T)$ measurements were performed by slowly lowering the temperature T of the system to reach equilibrium."
We found a linear variation of G_{dark} a function of T that comes from the linear approximation of the Arrhenius law between 200K and 300K of our previous article Gauvin et al[6].

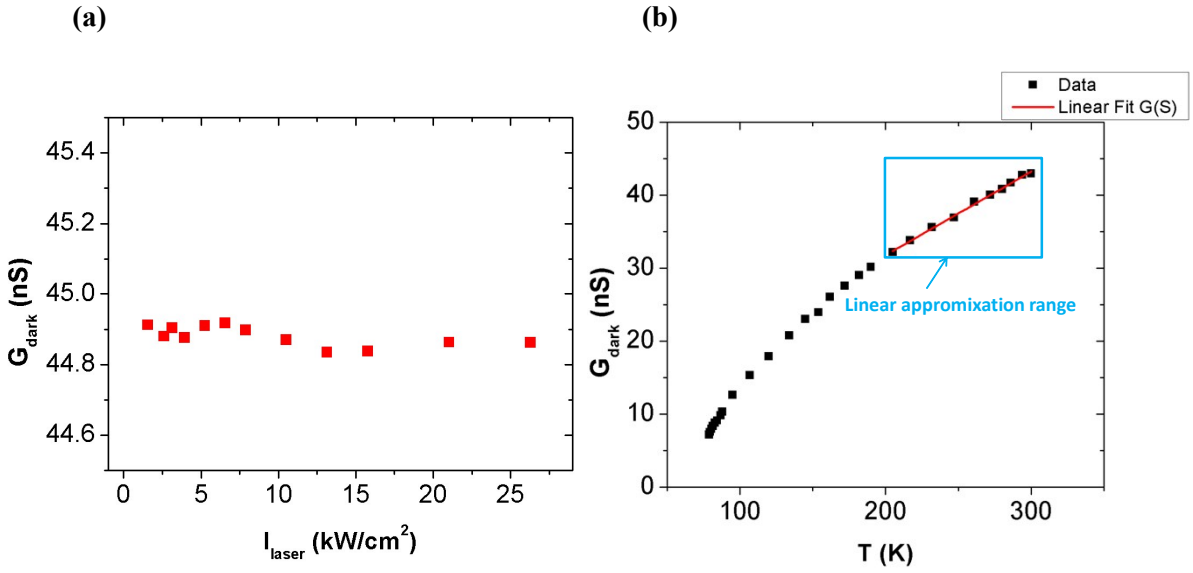

Figure S5: (a) Dark conductance baseline after increasing intensity of the irradiating laser (corresponding to figure 3b). Baseline stability is clearly evidenced. **(b)** Dark electrical conductance of 20µm freestanding monolayered Au NP membrane as a function of temperature. Black squares and red line indicate experimental data and the best fitted linear curve of G_{dark} vs. T in the 200-300K range.

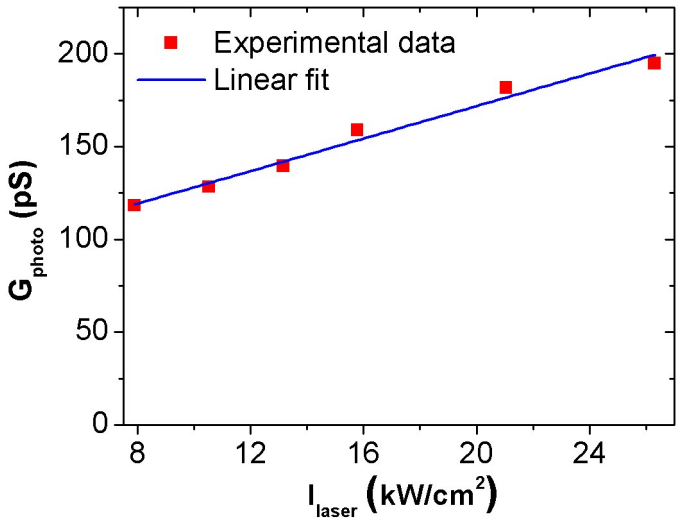

Figure S6: Plasmon-induced conductance G_{photo} as a function of illumination I_{Laser} in the bolometric part (high values of I_{laser}). G_{photo} data are indicated as red squares and the blue line is the best-fitted curve (R^2= 0.98) using Equation (2).

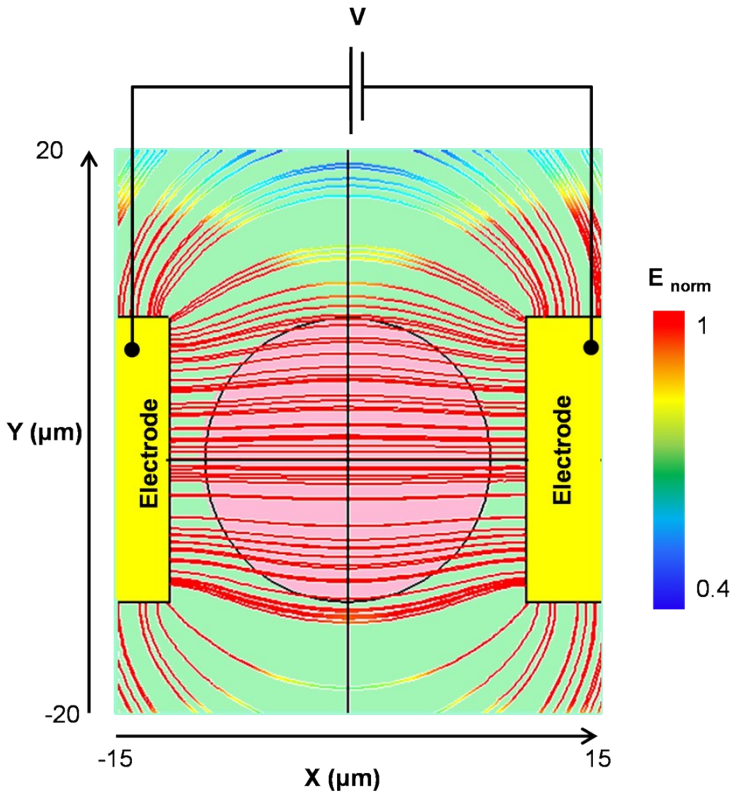

Figure S7: Simulated electric field lines within the gap between the polarized electrodes using finite element analysis. The normalized electric field amplitude E_{norm} is indicated by color-scale.

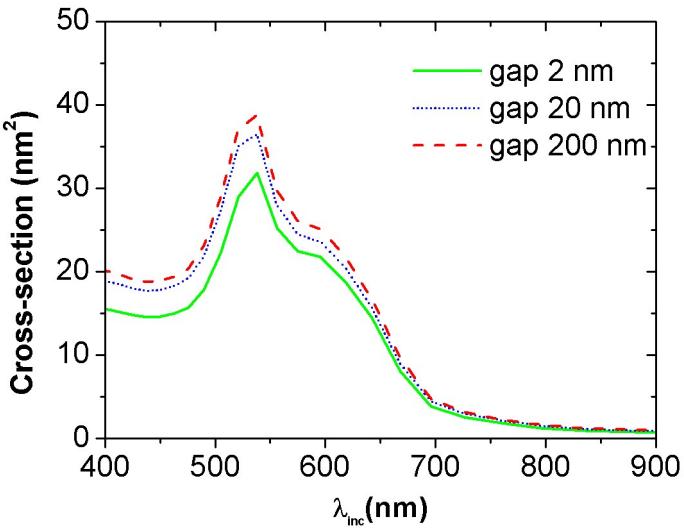

Figure S8: Absorption cross-section obtained by DDA simulations on a dimer of 7 nm Au NPs as a function of incident wavelength, calculated for different distances between a NP dimer and a 100 nm thick Si_3N_4 substrate.

REFERENCES

(1) Draine, B. T., 1988. "The Discrete-Dipole Approximation and its Application to Interstellar Graphite Grains". Astrophys. J., 333, 848–872.

(2) Goodman, J. J., Draine, B. T., & Flatau, P. J., 1990. "Application of fast-Fourier transform techniques to the discrete dipole approximation". Optics Letters, 16, 1198–1200.

(3) Draine, B. T. & Flatau, P. J., 1994. "Discrete-dipole approximation for scattering calculations". J. Opt. Soc. Am., 11, 1491–1499.

(4) Flatau, P. J. & Draine, B. T., 2012. "Fast near-field calculations in the discrete dipole approximation for regular rectilinear grids". Optics Express, 20, 1247–1252.

(5) Handbook of Optical Constants in Solids Edited by Edward D. Palik (c) Copyright 1985 by Academic press

(6) Gauvin, M.; Grisolia, J.; Alnasser, T.; Viallet, B.; Xie, S.; Brugger, J.; Ressier, L. "Electro-mechanical sensing in freestanding monolayered gold nanoparticle membranes." Nanoscale 2016 8 (22), 11363-11370